Front. Mech. Eng. 2017, 12(3): 406–419
DOI 10.1007/s11465-017-0419-0

RESEARCH ARTICLE

Yun KONG, Tianyang WANG, Zheng LI, Fulei CHU

Fault feature extraction of planet gear in wind turbine gearbox based on spectral kurtosis and time wavelet energy spectrum

Abstract Planetary transmission plays a vital role in wind turbine drivetrains, and its fault diagnosis has been an important and challenging issue. Owing to the complicated and coupled vibration source, time-variant vibration transfer path, and heavy background noise masking effect, the vibration signal of planet gear in wind turbine gearboxes exhibits several unique characteristics: Complex frequency components, low signal-to-noise ratio, and weak fault feature. In this sense, the periodic impulsive components induced by a localized defect are hard to extract, and the fault detection of planet gear in wind turbines remains to be a challenging research work. Aiming to extract the fault feature of planet gear effectively, we propose a novel feature extraction method based on spectral kurtosis and time wavelet energy spectrum (SK-TWES) in the paper. Firstly, the spectral kurtosis (SK) and kurtogram of raw vibration signals are computed and exploited to select the optimal filtering parameter for the subsequent band-pass filtering. Then, the band-pass filtering is applied to extrude periodic transient impulses using the optimal frequency band in which the corresponding SK value is maximal. Finally, the time wavelet energy spectrum analysis is performed on the filtered signal, selecting Morlet wavelet as the mother wavelet which possesses a high similarity to the impulsive components. The experimental signals collected from the wind turbine gearbox test rig demonstrate that the proposed method is effective at the feature extraction and fault diagnosis for the planet gear with a localized defect.

Keywords wind turbine, planet gear fault, feature extraction, spectral kurtosis, time wavelet energy spectrum

Received August 18, 2016; accepted November 18, 2016

Yun KONG, Tianyang WANG (✉), Zheng LI, Fulei CHU
Department of Mechanical Engineering, Tsinghua University, Beijing 100084, China
E-mail: wty19850925@126.com

1 Introduction

In view of global climate change and serious situation of energy security, wind power, as a representative of clean and highly-efficient energy source, is in the spotlight by virtue of its unique advantages of the vast reserve, pollution-free and being well-developed with sophisticated techniques [1]. With a large amount of wind farms built rapidly, numerous relevant issues appear in industrial applications of wind turbines, such as poor reliability, low efficiency, and high failure rate [2]. Moreover, as the most critical and vital components, the wind turbine gearbox remains the highest fault rate. Planetary stage transmission plays a vital role in wind turbine drivetrains for its large power transmission capacity in a relatively compact structure. In general, planetary gearboxes always work under harsh working conditions like heavy loads, wind gust, and dust corrosion. Thus, planetary gearboxes are often subject to potential damage, such as planet gear pitting, crack and even tooth breakage [3]. The faulty gearbox could lead to catastrophic failure of the entire transmission system, and massive investment and productivity losses consequently. Therefore, condition monitoring and fault diagnostics of the wind turbine gearboxes are valuable for both wind turbine industry and academic research.

Signatures of faulty wind turbine gearboxes can be reflected by vibratory, thermal, acoustic, electrical signals analysis and oil debris signature analysis [4–7]. Among these methodologies, vibration measurement has been proven to be one of the most effective and widely applied techniques [8]. The vibrations of planetary gearboxes are easily affected by the random alternating loads and their complicated excitations from the interior and exterior. Additionally, considering the influence of time variant vibration transfer path induced by their complex structure, the vibration signal of planetary gearbox exhibits several unique characteristics: Complex frequency components,

low signal-to-noise ratio, and weak fault feature [9]. Concerning the fault diagnosis for wind turbines, the most challenging work is the fault diagnosis for the planet gear. How to extract the weak fault feature and achieve precise incipient fault diagnosis for faulty planet gears, especially in the case of heavy noises and various modulation effects caused by time variant vibration transfer path, is a hot research topic and has been attracting increasing attention of academic researchers.

A local fault at the meshing gear contact surface often gives rise to the impulsive signature in the vibration signal. Meanwhile, due to continuously rotating of the machine, the impulsive components occur repetitively with a particular period. Hence, extracting the repetitive transients and identifying its frequency from the raw vibration signal facilitates to identify the occurrence of the abnormal condition of machine components correspondingly [10]. Such repetitive impulses usually locate in the high-frequency band which is closely related to the machine structure. Moreover, the local fault-induced transients are often contaminated by heavy noises and various interferences. A practical approach to periodic transient extraction is to filter the raw vibration signal through informative frequency band [11,12].

Spectral kurtosis (SK) has been extensively applied as a frequency band parameter indicator for band-pass filter design to extrude the non-Gaussian components. Antoni [13,14] proposed the formal definition of spectral kurtosis for non-stationary signals, using the World-Cramer decomposition and the paradigm of conditionally non-stationary processes. Further, Antoni and Randall [15] applied SK to provide a robust way of detecting incipient faults even in the presence of strong masking noise and introduced the concept of kurtogram to design optimal filters for filtering out the mechanical signature of faults. An adaptive SK technique was proposed to optimize filter bandwidth and center frequency by means of right-expanding an initial window in the frequency axis via successive attempts to merge it with its subsequent translated windows [16]. Barszcz and Randall [17] detected a tooth crack in the planetary gear of a wind turbine using the SK technique. An improved kurtogram method adopting wavelet packet transform as the filter of kurtogram was proposed to overcome the shortcomings of limited accuracy using the original kurtogram, and its improved performance was demonstrated by analyzing the collected vibration signal of rolling element bearings [18].

As one of the most powerful non-stationary signal processing methods, wavelet transform has been extensively studied and successfully applied in rotating machine fault diagnosis (RMFD). The applications of wavelet transform in RMFD could be categorized into the following aspects: Continuous wavelet transform-based fault diagnosis, discrete wavelet transform-based fault diagnosis, wavelet package transform-based fault diagnosis and second generation wavelet transform-based fault diagnosis [19]. Particularly, continuous wavelet transform has been widely applied for signal denoising and feature extraction of vibration signals, owing to its flexible selectivity of base wavelet function [20]. Morlet wavelet was selected as the mother wavelet and a denoising method based on continuous wavelet transform was applied to feature extraction of mechanical dynamical vibration signals [21]. A novel denoising method based on adaptive Morlet wavelet and singular value decomposition was exploited to extract feature for wind turbine vibration signal, and was proven to be an effective approach to detecting the impulsive components hidden in heavy, noisy vibratory signals [22].

In this paper, to address the problem that fault feature of planet gear in the wind turbine gearbox is too weak to extract, we propose a novel feature extraction method based on spectral kurtosis and time wavelet energy spectrum (SK-TWES). First, the kurtogram of the raw vibration signal is computed, and the optimal bandwidth and center frequency are determined according to the maximum SK value. Second, the bandpass filtering is performed to filter out the transient impulsive components, using the optimal frequency parameters. Then, we adapt continuous wavelet transform theory to propose the time wavelet energy spectrum analysis method, with the Morlet wavelet selected as the mother wavelet to realize the optimal matching with the impulsive components. After obtaining the time wavelet energy spectrum, we are expected to identify the prominent fault characteristic frequency. Finally, the experimental analyses of planet gear with a localized defect in the wind turbine gearbox are introduced to validate the effectiveness of the proposed method in this paper.

The remaining parts of the paper are organized as follows. In Section 2, the theoretical backgrounds of SK and time wavelet energy spectrum are given respectively, then the main procedures of the proposed feature extraction method are introduced in the subsequent subsection. In Section 3, the experiment setting about the wind turbine gearbox test rig is described in detail. In addition, the application of the proposed method to experimental vibration signal of planet gear with a localized fault is introduced; and some comparative analyses with other conventional feature extraction methods are given. Finally, the conclusions are drawn in Section 4.

2 Proposal of feature extraction method based on SK-TWES

2.1 Spectral kurtosis and kurtogram

To supplement the classical power spectral density which

cannot detect and characterize transients in a non-stationary signal, Dwyer [23] originally devised the SK. The idea of SK is basically to compute the kurtosis at "each frequency line" to discover the presence of hidden non-stationaries and to indicate their locations in the frequency domain. Therefore, the SK can indicate how the impulsiveness of a conditionally non-stationary (CNS) process varies with the frequency, and it has been extensively applied to extract the transients out of mechanical dynamical faulty vibration signal [24].

Based on the Wold-Cramer decomposition, any non-stationary stochastic process $Y(t)$ can be described as the output of a linear, casual, time-variant system excited by non-stationary signal $X(t)$ [13]:

$$Y(t)=\int_{-\infty}^{+\infty}\mathrm{e}^{j2\pi ft}H(t,f)\mathrm{d}X(f), \tag{1}$$

where $H(t,f)$ is the Fourier transform of the time-varying impulse response $h(t,s)$, $\mathrm{d}X(f)$ is an orthogonal spectral process associated with $X(t)$.

The SK is defined under the assumption that the process is conditionally non-stationary. In this case, the fourth-order spectral cumulant $C_{4Y}(f)$ of a CNS process can be defined as

$$C_{4Y}(f)=S_{4Y}(f)-2S_{2Y}^2(f),\ f\neq 0, \tag{2}$$

where $S_{2nY}(f)$ ($n=1, 2, 3, \ldots$) is the $2n$-order instantaneous spectral moment, it is a measure of the energy of complex envelope and given by

$$S_{2nY}(f)\triangleq E\{S_{2nY}(t,f)\}=E\{|H(t,f)\mathrm{d}X(f)|^{2n}\}/\mathrm{d}f$$

$$=E\{|H(t,f)|^{2n}\}S_{2nX}(f), \tag{3}$$

with $E\{\cdot\}$ standing for the time-average operator.

The energy-normalized fourth-order spectral cumulant of a CNS process is defined as SK, which gives a measure of the peakiness of the probability density function of a CNS process at frequency f.

$$K_Y(f)=\frac{C_{4Y}(f)}{S_{2Y}^2(f)}=\frac{S_{4Y}(f)}{S_{2Y}^2(f)}-2,\ f\neq 0. \tag{4}$$

Another important tool based on SK is the kurtogram, which presents SK values calculated for various parameters of bandwidth and center frequency. It is proposed as the tool for identification of detection filters. The original kurtogram is firstly calculated based on short time Fourier transform. Afterward, the filter bank approach is proposed to obtain the fast kurtogram, which requires less computation time and gives results on the same level of quality [14]. In this paper, the filter bank approach is used to compute the kurtogram and the program for implementing the calculation for the fast kurtogram is downloaded from Ref. [25] provided by J. Antoni.

2.2 Time wavelet energy spectrum analysis

2.2.1 Continuous wavelet transform

The wavelet transform of signal $x(t)$ is defined as the inner product of the signal and the wavelets in the Hilbert space of the L^2 norm, namely, it utilizes a series of oscillating functions $\psi_{a,b}(t)$ with different frequencies as window functions to scan and translate the signal of $x(t)$, shown in the following form

$$\begin{aligned}W_x(a,b)&=\langle\psi_{a,b}(t),x(t)\rangle=\int_{-\infty}^{\infty}x(t)\psi_{a,b}^*(t)\mathrm{d}t\\&=\frac{1}{\sqrt{a}}\int_{-\infty}^{\infty}x(t)\psi^*\left(\frac{t-b}{a}\right)\mathrm{d}t,\ a>0,\end{aligned} \tag{5}$$

where $W_x(a,b)$ is wavelet coefficient which measures the similarity between the signal $x(t)$ and the mother wavelet $\psi_{a,b}(t)$, $\psi(t)$ is the mother wavelet, a is the scale factor, and b defines a translation factor of the wavelet.

Wavelet transform has an adaptable time-frequency resolution and its resolution depends on the frequency of the signal of interest, which reinforces its important status in the fault diagnostics field. According to the convolution properties of Fourier transform, Eq. (5) can also be represented as

$$W_x(a,b)=\sqrt{a}F^{-1}\{X(f)\hat{\psi}^*(af)\}, \tag{6}$$

where $X(f)$ and $\hat{\psi}^*(f)$ are the Fourier transform of $x(t)$ and $\psi^*(t)$, respectively, the asterisk stands for the complex conjugate, and F^{-1} denotes the inverse Fourier transform. In this sense, the selected mother wavelet functions are bandpass filters which are oscillatory in the time domain.

Additionally, the mother wavelet function $\psi(t)$ is assumed to lie in $L^2(C)$ and satisfy the admissibility condition

$$C_\psi=\int_{-\infty}^{\infty}|\hat{\psi}(\omega)|^2/|\omega|\mathrm{d}\omega<+\infty, \tag{7}$$

where $L^2(C)$ is the space of square integrable complex function.

2.2.2 Morlet wavelet

As for many mechanical dynamical signals, the periodic impulsive component is always the symptoms of faults. Therefore, it is vital to select a proper mother wavelet function similar to the impulsive components. In this paper, complex Morlet wavelet is used, expressed as follows [26]

$$\psi(t)=\pi^{-1/4}(\mathrm{e}^{-j\omega_0 t}-\mathrm{e}^{-\omega_0{}^2/2})\mathrm{e}^{-t^2/2}. \tag{8}$$

When $\omega_0\geqslant 5$, $\mathrm{e}^{-\omega_0{}^2/2}\approx 0$, the Morlet wavelet can be simplified in the following form:

$$\psi(t) = \pi^{-1/4} e^{-j\omega_0 t} e^{-t^2/2}. \quad (9)$$

Considering the Morlet wavelet function is a cosine signal decaying exponentially on both sides in the time domain (not considering the imaginary part of the complex Morlet wavelet function), it appears like an impulse component, which demonstrates that the continuous wavelet transform based on Morlet wavelet will have a high potential for feature extraction in machine fault diagnosis applications.

2.2.3 Time wavelet energy spectrum

The continuous wavelet transform possesses the energy preservation property, i.e., the Parseval equation, which can be described in the form:

$$\int_{-\infty}^{\infty} |x(t)|^2 \mathrm{d}t = \frac{1}{C_\psi} \int_{-\infty}^{\infty} \int_{-\infty}^{\infty} \frac{|W_x(a,b)|^2}{a^2} \mathrm{d}a\mathrm{d}b. \quad (10)$$

According to Eq. (10), the left part of the equation represents the energy of signal $x(t)$. Thus, $|W_x(a,b)|^2/(C_\psi a^2)$ can stand for the energy density function which describes the distribution of energy in (a, b) plane. Further, Eq. (10) can be rewritten as the integration of time wavelet energy function $E(b)$ along the axis of translation parameter b in the following form.

$$\int_{-\infty}^{\infty} |x(t)|^2 \mathrm{d}t = \int_{-\infty}^{\infty} E(b) \mathrm{d}b, \quad (11)$$

$$E(b) = \frac{1}{C_\psi} \int_{-\infty}^{\infty} \frac{|W_x(a,b)|^2}{a^2} \mathrm{d}a, \quad (12)$$

where $E(b)$ gives the signal energy's distribution with time varying, and it is so called as the time wavelet energy distribution function.

Obviously, the impulse signal which occurs at a certain moment in the time domain is equally stretched in the whole frequency domain. Therefore, by means of integrating the energy density function along the scale (frequency) axis a, the distribution of signal energy with time varying can be obtained and contributes to identifying the time location of impulse occurrence. Furthermore, we can obtain the time wavelet energy spectrum $ES(f)$ to acquire the repetitive frequency of periodic impulsive components, which is deduced by the Fourier analysis of time wavelet energy distribution function $E(b)$. The time wavelet energy spectrum $ES(f)$ and its discretization form $ES(k)$ are expressed as follows.

$$ES(f) = \int_{-\infty}^{+\infty} E(b) e^{-j2fb} \mathrm{d}b, \quad (13)$$

$$ES(k) = \sum_{n=0}^{N-1} E(n) \exp\left(-j\frac{2\pi}{N} nk\right). \quad (14)$$

Consequently, the time wavelet energy spectrum is capable of identifying the frequency of periodic impulsive components, and fault diagnosis can be achieved using this approach, combined with the fault characteristic frequency of various machine components such as bearings and gears.

2.3 The proposed method of feature extraction based on SK-TWES

Motivated by the advantages of kurtogram and the proposed time wavelet energy spectrum approach, a novel feature extraction method based on SK-TWES is proposed in the paper, and its main procedures are illustrated in Fig. 1 and the concrete steps for fault feature extraction of planet gear using the proposed method based on SK-TWES are also provided as follows:

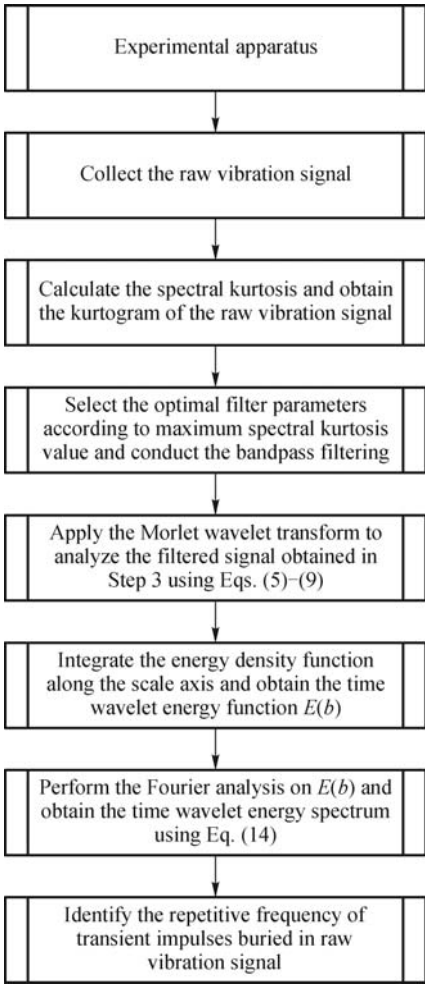

Fig. 1 Flowchart of the proposed feature extraction method based on SK-TWES

Step 1: Collect the raw vibration signal (in the experimental validations of this paper, we collect the vibration signal of one planet gear with a localized fault and healthy

planet gears in the wind turbine gearbox test rig, respectively).

Step 2: Calculate SK of the filtered vibration signals with various center frequency and bandwidth using the filter bank approach, and obtain the kurtogram of the raw vibration signal measured in Step 1.

Step 3: Select the optimal filter parameters including the center frequency and bandwidth, which correspond to the maximum spectral kurtosis value in the kurtogram derived in Step 2, and then utilize them to design a bandpass filter to preliminarily filter out the periodic transient impulse components from the raw vibration signal measured in Step 1.

Step 4: Apply the Morlet wavelet transform to analyze the filtered signal obtained in Step 3 using Eqs. (5)–(9), and obtain the wavelet coefficients $W_x(a,b)$.

Step 5: Integrate the energy density function $|W_x(a,b)|^2/(C_\psi a^2)$ along the scale axis and obtain the time wavelet energy function $E(b)$ using Eq. (12), for the purpose of further extruding the impulsive components. Then, we conduct the Fourier analysis to the time wavelet energy distribution function $E(b)$ and obtain the time wavelet energy spectrum $ES(k)$ using Eq. (14).

Step 6: Identify the repetitive frequency of transient impulses to implement the fault diagnosis of machine components, from the time wavelet energy spectrum.

3 Experimental signal analysis

In this section, we analyze the experimental signal with healthy planet gears and signal with a damaged planet gear in the wind turbine gearbox test rig, respectively, which are measured at the Machinery Dynamics and Fault Diagnostics Laboratory at Tsinghua University, to validate the effectiveness of the proposed method.

3.1 Experiment settings

The vibration measurement experiment with a localized planet gear fault is conducted in the wind turbine gearbox test rig illustrated in Fig. 2. The wind turbine gearbox test rig has the same configurations as one of the actual gearbox applied in the practical wind power generation, except its equally shrunken size. It mainly consists of six parts: Two wind turbine gearboxes mounted symmetrically and inversely, loader, loading motor, cooling system, variable frequency controller, and alternating current (AC) motor. In our test rig, the variable frequency controller is utilized to change the rotating speed of AC motor by varying the frequency of power source. The load is applied to the output shaft by means of loading motor injecting high-pressure oil into the loader which is connected with the output shaft of the gearbox. The right gearbox decreases the rotating speed of AC motor, whereas the left gearbox increases the rotating speed and is installed to simulate both the normal and faulty wind turbine gearbox with various configurations, respectively.

The wind turbine gearbox is composed of one planetary transmission stage (low-speed stage) and two parallel transmission stages (middle- and high-speed stages). The sketch map of transmitting routine in the wind turbine gearbox are shown in Fig. 3. Table 1 lists the gear parameters of the wind turbine gearbox.

As for the experimental operating condition when the gearbox is assembled with seeded planet gear tooth breakage, the variable frequency controller is set as 50 Hz, correspondingly, and the AC motor spindle is constantly rotating at 1492 r/min with small fluctuation shown in Fig. 4(c); and the pressure of oil injected into the

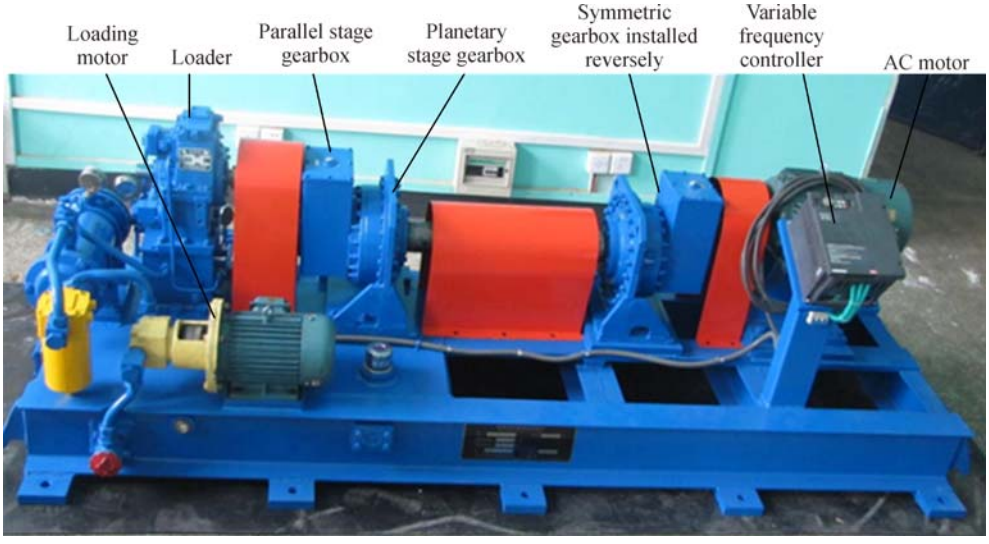

Fig. 2 Wind turbine gearbox test rig for fault diagnosis

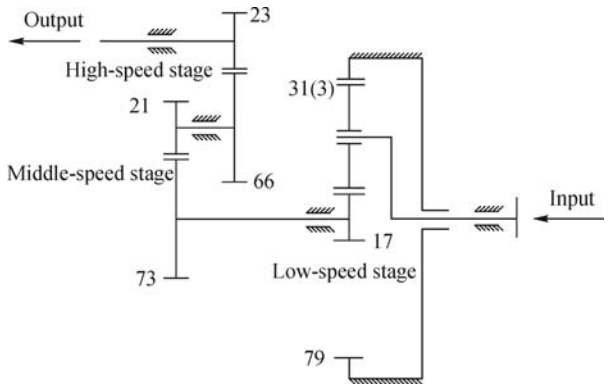

Fig. 3 Transmitting routine in wind turbine gearbox

loader pump is as high as 0.15 MPa. The vibration signals of the wind turbine gearbox with tooth breakage in a planet gear (shown in Fig. 4(a)) are acquired by accelerometers mounted on the casing of the supporting bearing of the sun gear, and the sampling rate is 16384 Hz. The installing location of accelerometers is illustrated in Fig. 4(b) and the specifications about the accelerometers are listed in Table 2. In contrast, the baseline data is also collected as a reference when the wind turbine gearbox operates in a healthy condition. This measurement is performed when the AC motor spindle rotates at constant speed 1478 r/min

Table 1 Parameters of gears in the wind turbine gearbox

Stage	Gear type	Tooth number
Low-speed	Sun gear	17
	Planet gear	31(3)
	Ring gear	79
Middle-speed	Gear	73
	Pinion	21
High-speed	Gear	66
	Pinion	23

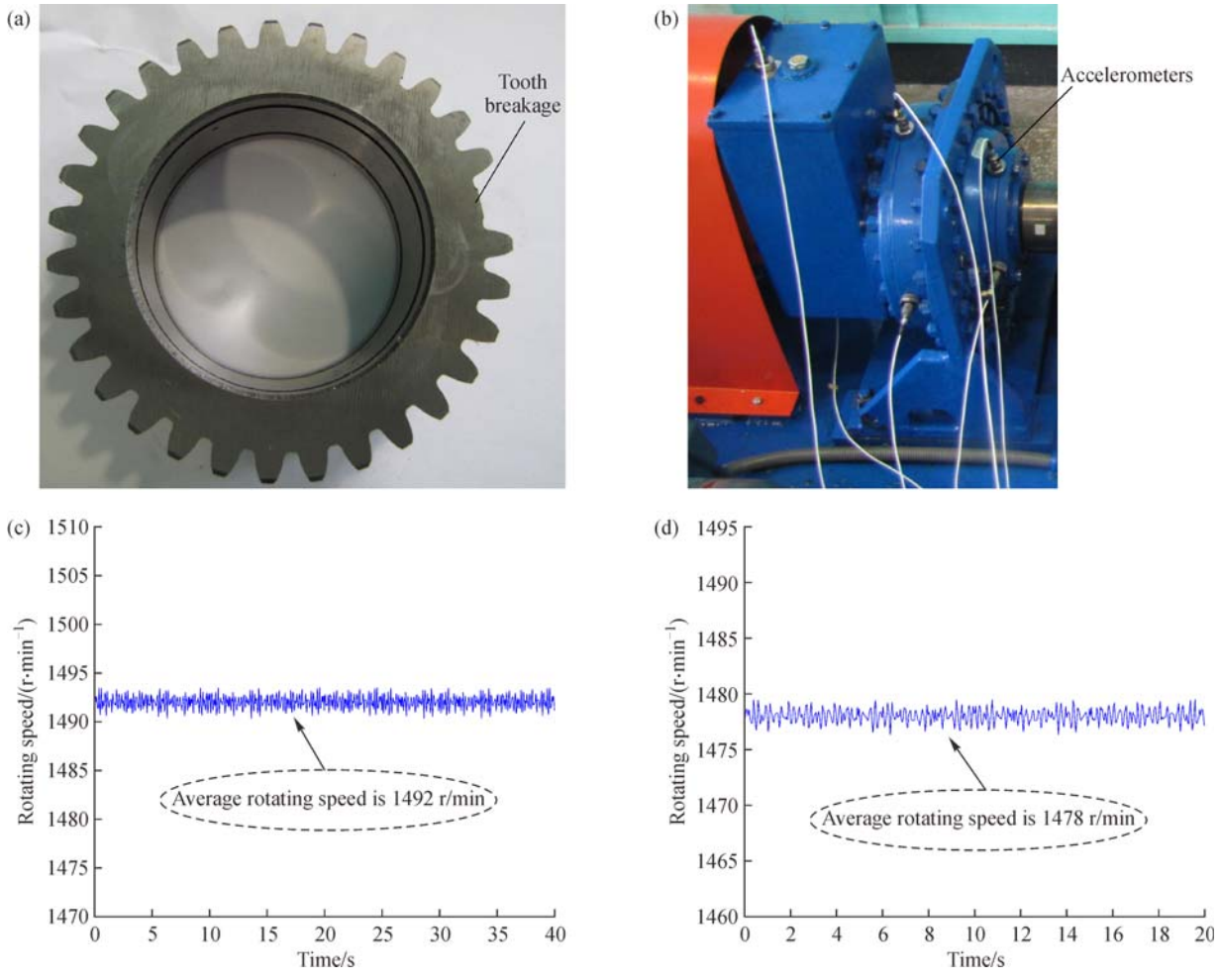

Fig. 4 (a) Planet gear with tooth breakage; (b) acceleration sensors placement; the rotating speed of AC motor: (c) Experiment on faulty wind turbine gearbox; (d) experiment on healthy wind turbine gearbox

Table 2 Specifications about the accelerometers

Manufacturer	Model	Sensitivity/(mV·g^{-1})	F.S. range/g	Frequency range (±5%)/Hz	Linearity
DYTRAN INST Inc.	3056B1	10	±500	1–10000	±1%

with small fluctuation shown in Fig. 4(d), and other operating condition is the same as the case with planet gear tooth breakage.

The characteristic frequencies of the wind turbine gearbox include the meshing frequency of each meshing pair, rotating frequency of each shaft, and characteristic frequency of gears with a localized defect. The characteristic frequency of gears is very crucial to its fault diagnosis, which refers to how many times its faulty tooth meshes with the mating gear(s) per second [3]. For the fixed-axis gearboxes, the characteristic frequency of gear with localized fault is the rotating frequency of the gear of interest. As for planetary gearboxes, the characteristic frequency of gears depends on not only the gearbox running speed but also its configuration, such as the number of planet gears and the tooth number of each gear.

According to the wind turbine gearbox configurations (see Table 1) and the rotating speed of AC motor shaft 1496 r/min when the gearbox is assembled with seeded planet gear tooth breakage fault, the characteristic frequencies in the wind turbine gearbox can be calculated [3,9], as listed in Table 3. f_{mi} represents the meshing frequency of the ith stage gear transmission; f_{pf} stands for the localized fault characteristic frequency of planet gear; f_{il} and f_{ih} is the rotating frequency of the low-speed shaft or high-speed shaft in the ith stage gear transmission; f_{ilf} and f_{ihf} is the localized fault characteristic frequency of gears installed on the low-speed shaft or high-speed shaft in the ith stage gear transmission.

Table 3 Characteristic frequency in the wind turbine gearbox test rig

Stage	Characteristic frequency	Value/Hz
Low-speed	f_{m1}	34.874
	f_s	2.493
	f_c	0.441
	f_p	0.684
	f_{pf}	1.125
Middle-speed	f_{m2}	181.980
	f_{2l}	2.493
	f_{2h}	8.667
	f_{2lf}	2.493
	f_{2hf}	8.667
High-speed	f_{m3}	571.930
	f_{3l}	8.667
	f_{3h}	24.867
	f_{3lf}	8.667
	f_{3hf}	24.867

3.2 Signal analysis based on the SK-TWES

To validate the performance of the feature extraction method based on the spectral kurtosis and time wavelet energy spectrum, we analyze the experimental vibration signals collected from the wind turbine gearbox test rig with a faulty planet gear and healthy gears simultaneously.

From Fig. 5(a), it can be seen that some impulses occur compared to the signals collected when the gearbox is healthy in Fig. 5(c), but the periodic impulsive components are contaminated by heavy noises, thus the period of the impulsive components are too obscure to identify directly. According to the spectrum of the raw vibration signal shown in Figs. 5(b) and 5(d), it reveals that the frequency components are extraordinarily complicated, and the planetary stage meshing frequency along with its sidebands can even be negligible. Because the planetary gear transmission operates at very low speed compared with the parallel high-speed stage gear transmission, and various amplitude modulations or frequency modulations interference the signal acquired by the accelerometer due to the complex motion of planet gear, time varying vibration transfer path, and the various vibration sources coupling with each other.

We take a zoom-in picture of the spectrum of the raw vibration signal in the low frequency region, to deeply understand the dominant frequency components. The result in Fig. 5(b) shows that two times the frequency f_{3h} 49.73 Hz and its harmonic frequencies nf_{3h} (74.6, 99.45 Hz, etc.) dominate the spectrum, which may demonstrate that the high-speed output shaft is misaligned. The similar frequency components can be also observed in the case with healthy gears shown in Fig. 5(d), but its amplitude is relatively lower than other prominent frequency peaks. Unfortunately, the misalignment of the high-speed output shaft is inevitable in the laboratory section, which results in the harmonic interference to the detection of transient impulse, and affects the diagnosis accuracy of gear faults consequently.

Based on the procedures of the proposed feature extraction method, the kurtogram of the raw signal is then computed using the filter bank approach [25], and shown in Fig. 6(a). From Fig. 6(a), the frequency region which possesses the maximum SK value is marked with red dotted rectangle, and the optimal center frequency and bandwidth are selected as 7338.67 and 341.3 Hz,

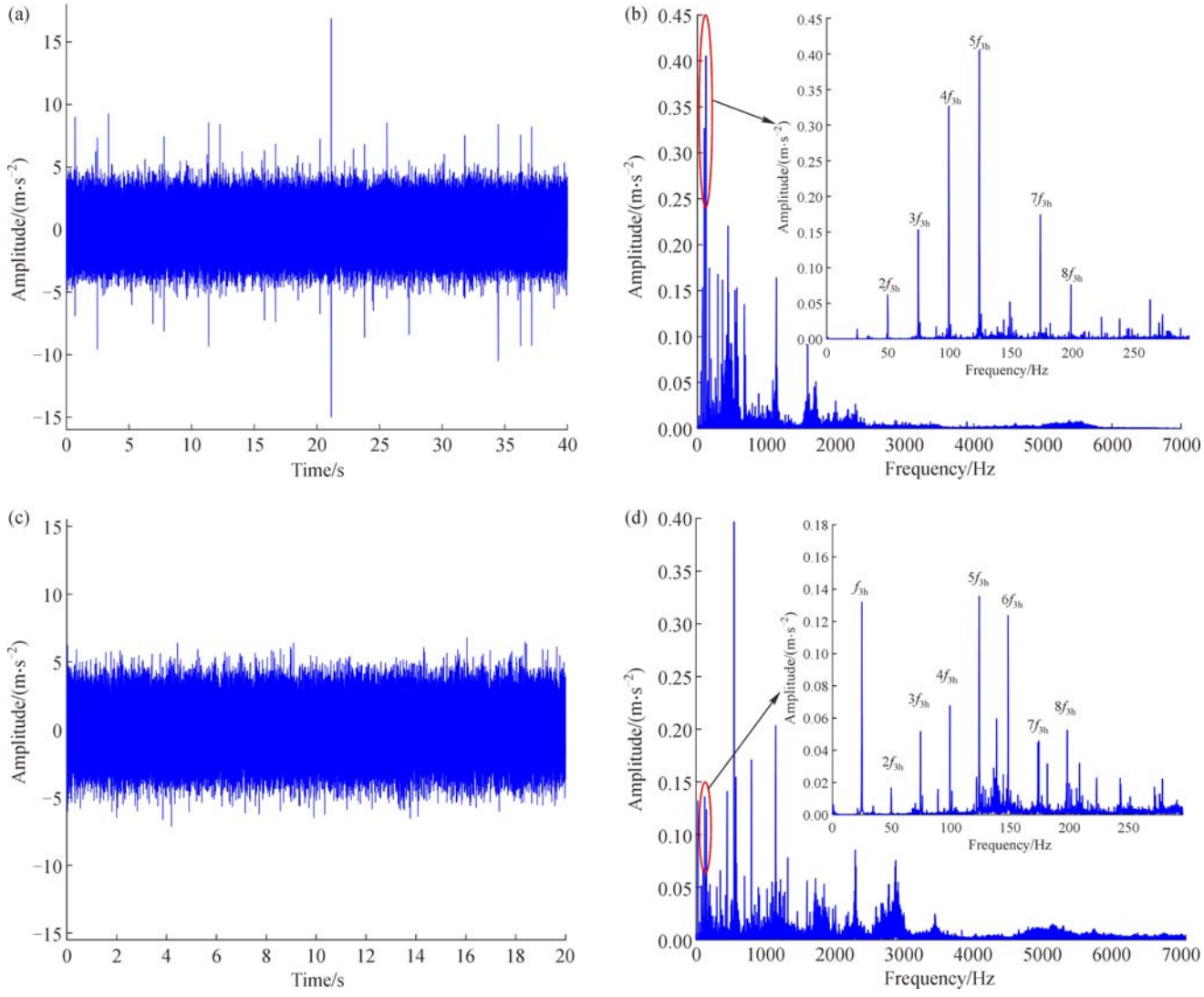

Fig. 5 Raw vibration signal for planet gear with localized fault: (a) Waveform and (b) spectrum; raw vibration signal for healthy planet gear: (c) Waveform and (d) spectrum

respectively. Then an optimal bandpass filter can be designed according to the selected optimal center frequency and bandwidth. Besides, the envelope of the bandpass filtered signal is also illustrated in Fig. 6(b). In the same way, we consider the case with healthy planet gears for comparison, the kurtogram and the envelope signal after filtering operation based on the optimal filter parameters obtained in the kurtogram are also computed and shown in Figs. 6(c) and 6(d), respectively.

In Fig. 6(b), we can observe that although the transient impulses are extruded in the time domain and more prominent than the healthy case shown in Fig. 6(d), the period of transient impulses is still not clear and apparent. To extract the periodic impulsive components further and identify the repetitive frequency, we apply the time wavelet energy spectrum analysis to the filtered signal, and the obtained time wavelet energy spectrum is illustrated in Fig. 7.

In Fig. 7(a), the fault characteristic frequency of planet gear f_{pf} 1.125 Hz and its harmonic frequencies nf_{pf} dominate the time wavelet energy spectrum of the filtered signal. Namely, the repetitive frequency of periodic transient impulsive components is successfully identified. Considering the case with healthy planet gears, Fig. 7(b) shows that the time wavelet energy spectrum is dominated by three times of carrier rotating frequency $3f_{\mathrm{c}}$ and the rotating frequency of the high-speed and the middle shaft $f_{3\mathrm{h}}$, $f_{3\mathrm{l}}$. These dominant frequency components are irrelevant to the planet gear fault.

To ensure the high precision and reliable validation of our proposed method in the experimental applications, another two measurements were performed on the same

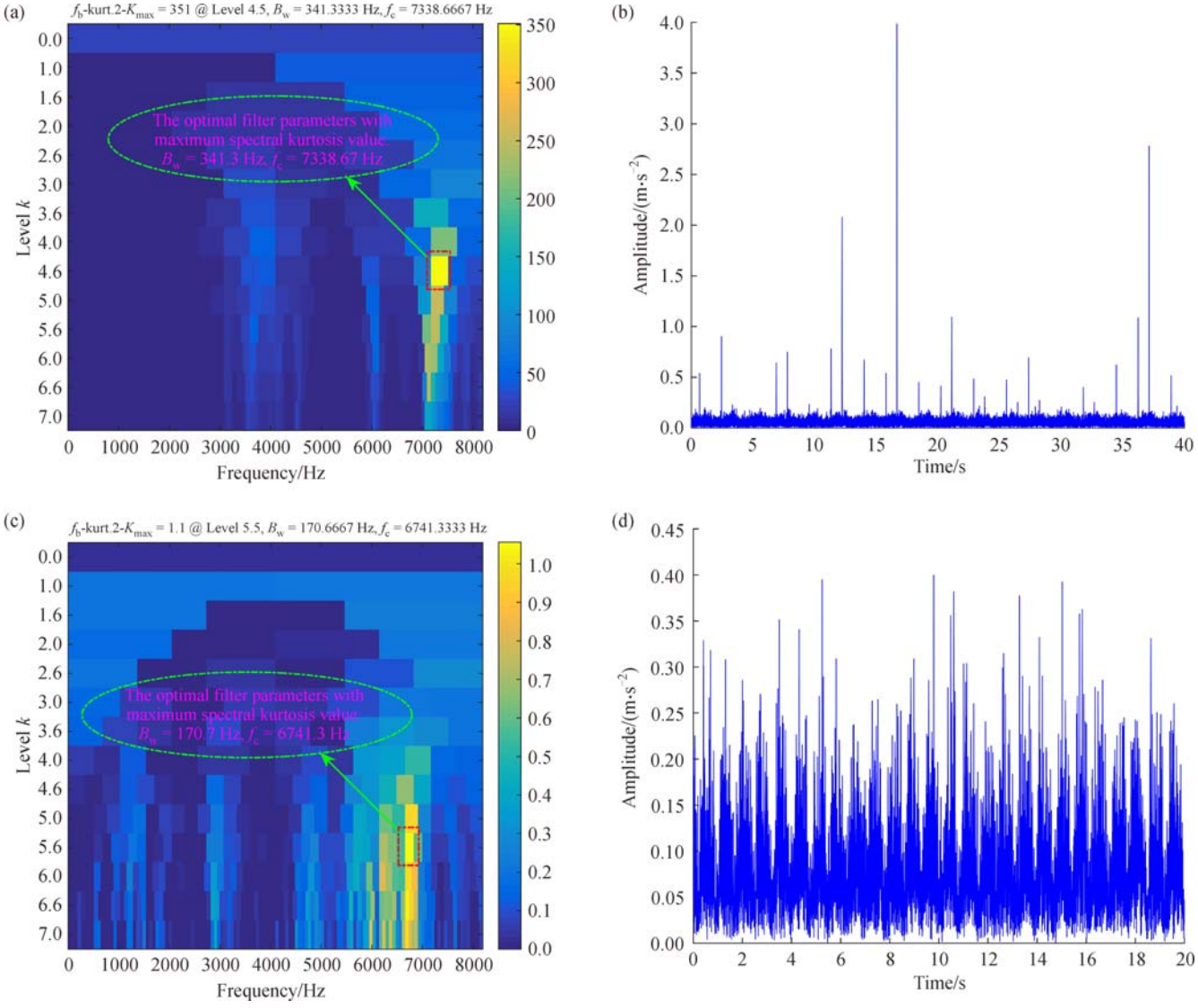

Fig. 6 Planet gear with a localized fault: (a) Kurtogram, (b) envelope of filtered signal based on kurtogram; healthy planet gears: (c) Kurtogram, (d) envelope of filtered signal based on kurtogram

operating condition, and the relevant results using our proposed method and comparative methods are provided in the Appendix.

To conclude, the repetitive impulse induced by tooth breakage fault in a planet gear is still very obscure and its fault characteristic frequency is hard to identify, due to various demodulations and the strong interferences from two parallel gear transmissions whose vibration level is much higher than that of the planetary gear transmission. The effectiveness of our proposed method based on SK-TWES is verified by the experimental signal. Thus, the proposed method realizes the fault diagnosis for planet gear with a localized defect in the wind turbine gearbox effectively.

3.3 Comparative analyses

In Section 3.2, the effectiveness of the proposed feature extraction method based on SK and time wavelet energy spectrum are validated by analyzing the experimental vibration signal of planet gear with a local defect in the wind turbine gearbox test rig. Furthermore, the following comparative analyses are conducted with the conventional envelope demodulation analysis, the envelope demodulation combined with the kurtogram, and the time wavelet energy spectrum analysis without any preprocessing approach. These results of comparative studies are illustrated in Figs. 8(a)–8(c).

Envelope demodulation analysis is a powerful technique

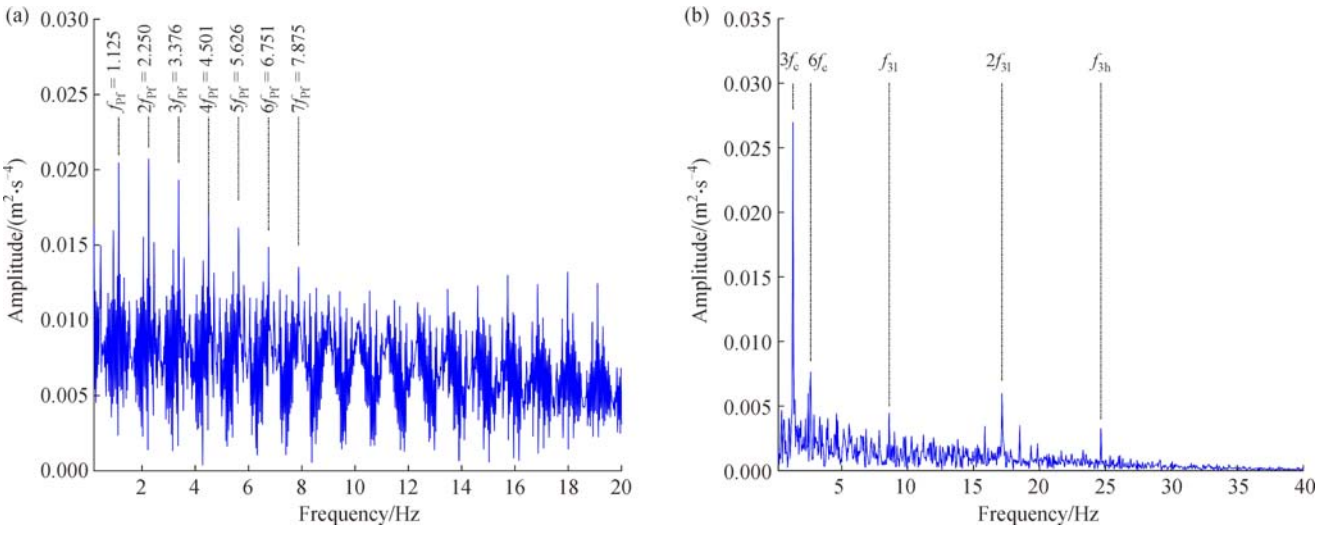

Fig. 7 Time wavelet energy spectrum of filtered signal: (a) Planet gear with a localized fault; (b) healthy planet gears

and extensively applied to detect the impulsive components in cases with high signal-to-noise ratio, such as the vibration signal of rolling element bearings with race defect. Meanwhile, it has a high capability of demodulating the amplitude modulation signal. The squared envelope spectrum consists of three steps in general: First, obtain the analytic signal $z(t)$ of real signal $x(t)$ using the Hilbert transform which is essentially defined as the convolution of real signal with $1/\pi t$ as the following equation,

$$y(t) = \frac{1}{\pi}\int_{-\infty}^{+\infty}\frac{x(\tau)}{t-\tau}\mathrm{d}\tau, \tag{15}$$

$$z(t) = x(t) + iy(t) = a(t)\mathrm{e}^{i\varphi(t)}. \tag{16}$$

Second, coupling the $x(t)$ and $y(t)$ in Eqs. (15) and (16), we can calculate the instantaneous amplitude $a(t)$ and instantaneous phase $\varphi(t)$ of real signal $x(t)$ in the following form

$$a(t) = \sqrt{x^2(t) + y^2(t)},\ \varphi(t) = \arctan(y(t)/x(t)). \tag{17}$$

Third, by performing the spectrum analysis on the squared envelope $a^2(t)$ (namely, the square of instantaneous amplitude of signal $x(t)$), we can obtain the squared envelope spectrum.

However, the result of squared envelope spectrum of the measured raw signal in Fig. 8(a), shows that the conventional envelope demodulation analysis fails to identify the repetitive frequency of impulsive components hidden in the noisy vibration signal, and the frequency f_{3l} 8.67 Hz, f_{3h} 24.87 Hz and their multiple frequencies nf_{3l}, nf_{3h} dominate the squared envelope spectrum. The result demonstrates that the modulations induced by the f_{3l} and f_{3h} are evident and interference the detection of transient impulses produced by localized planet fault in the wind turbine gearbox.

Envelope demodulation combined with bandpass filtering based on the kurtogram is a very attractive approach for the feature extraction of impulsive components as well. The kurtogram first provides the optimal filter parameters for detecting the transients hidden in the noisy signal; then envelope demodulation is applied to analyze the filtered signal. From the squared envelope spectrum of the filtered signal in Fig. 8(b), the fault characteristic frequency of planet gear f_{pf} 1.125 Hz and its harmonic frequencies nf_{pf} is prominent, but the existed deficiencies are as follows: 1) The frequency offset component is significant, and the signal-to-noise ratio in Fig. 8(b) is much lower than that of Fig. 7(a); 2) the interference caused by the carrier rotating frequency component f_c 0.45 Hz is apparent as well. The two efficiencies may interrupt the precise fault diagnosis for planet gear with a local defect.

The time wavelet energy spectrum analysis without any preprocessing approach is intended to validate the powerfulness of spectral kurtosis to determine the optimal frequency band in which the impulsive components locate. In Fig. 8(c), the prominent frequencies are still the shaft rotating frequency of the high-speed stage f_{3l}, f_{3h}, and their multiples. Thus, the time wavelet energy spectrum without any preprocessing approach cannot effectively implement the feature extraction for planet gear with a local defect in the wind turbine gearbox test rig.

To sum up, the proposed feature extraction method based on SK-TWES has better performance at feature extraction of faulty planet gear, compared with the other three comparative methods. By applying the novel method to analyze the experimental vibration signal of planet gear with a localized fault, it is demonstrated that the proposed method is not only capable of extracting the repetitive

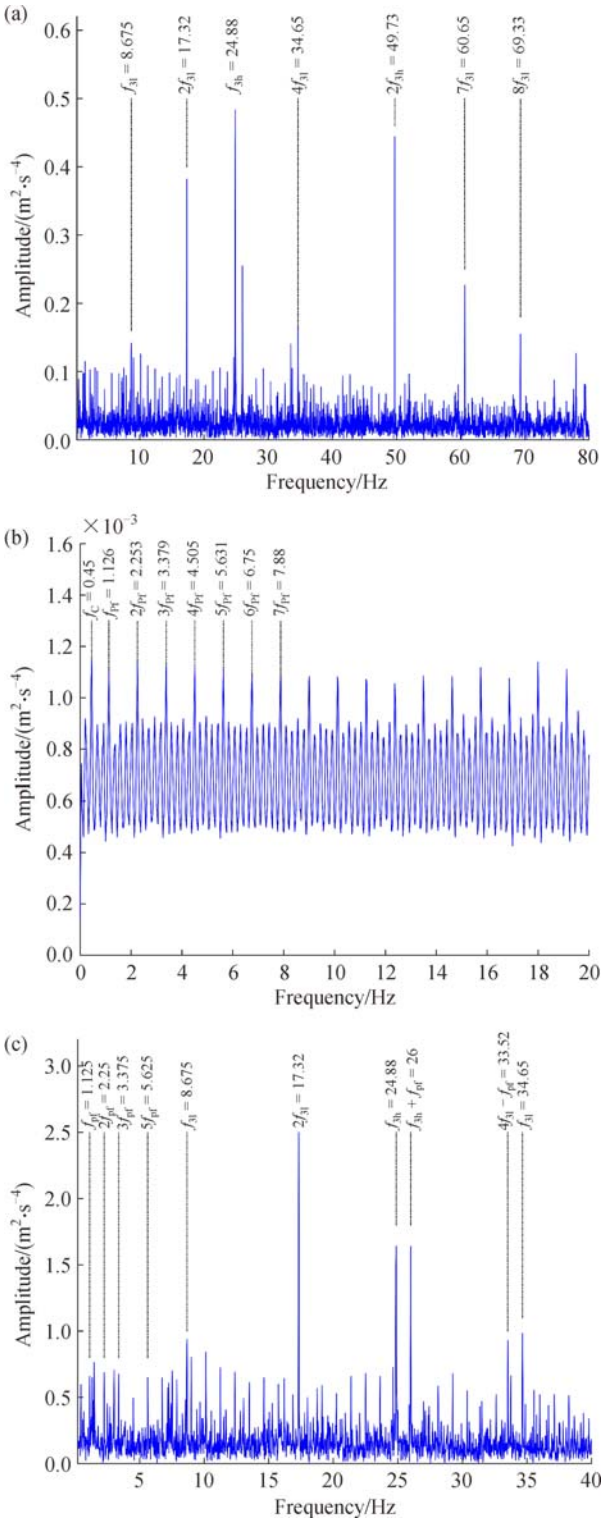

Fig. 8 Results of comparative studies: (a) The squared envelope spectrum of raw vibration signals; (b) the squared envelope spectrum of the filtered signal based on kurtogram; (c) the time wavelet energy spectrum without any preprocessing approach

impulsive transients and identifying its frequency but also robust to the strong noise masking effect and harmonic interferences from high-speed transmission stages.

4 Conclusions

In this paper, we propose a novel feature extraction method based on SK-TWES to overcome the deficiencies of existing methods when extracting the fault feature of planet gear with the localized defect. This approach combines the SK-TWES analysis to enhance and extract a better planet gear fault feature, i.e., the fault characteristic frequency. The proposed method mainly considers that the SK is sensitive to non-Gaussian transients in the non-stationary signal, thus the kurtogram is exploited to facilitate the design of optimal bandpass filter. Furthermore, Morlet wavelet is selected as the mother wavelet due to its high similarity to the impulsive component, and the time wavelet energy spectrum analysis based on continuous wavelet transform is introduced to identify the repetitive frequency of impulses immersed in the noisy signal. The experimental vibration signal of planet gear with a localized fault in the wind turbine gearbox is used to verify the effectiveness of the proposed approach. The results demonstrate that the prominent fault characteristic frequency and its harmonic frequency components are clear, and the harmonic interferences induced by high-speed transmission stages are well eliminated. Meanwhile, the conventional envelope demodulation techniques and time wavelet energy spectrum analysis without any preprocessing approach, do not behave well in this experimental application. Thus, the method based on SK-TWES is proven to be a reliable and potential tool for extracting the weak fault feature from various noises and interferences, and it has superiority over the aforementioned conventional approaches, particularly for the fault diagnosis of planet gear with a local defect in wind turbine gearboxes.

However, our proposed method based on SK-TWES still has a limited capability to extract the fault feature for planet gear with incipient pitting or crack defect. The authors will investigate the issues in their future research work.

Acknowledgements The authors gratefully appreciate all the reviewers and the editor for their valuable comments and advices about our manuscript. The authors gratefully acknowledge the support of this research work by the National Natural Science Foundation of China (Grant No. 51335006).

Appendix

In this appendix, we supplement another two measurements collected from the wind turbine gearbox test rig with tooth breakage in a planet gear, the operating condition is the same as what we have described before. The relevant results using the proposed method and the comparative methods are illustrated in the following Figs. A1 and A2. Both of the two repetitive experiments and the corresponding results demonstrate the effectiveness of our proposed method based on SK-TWES and its superiority over the comparative methods.

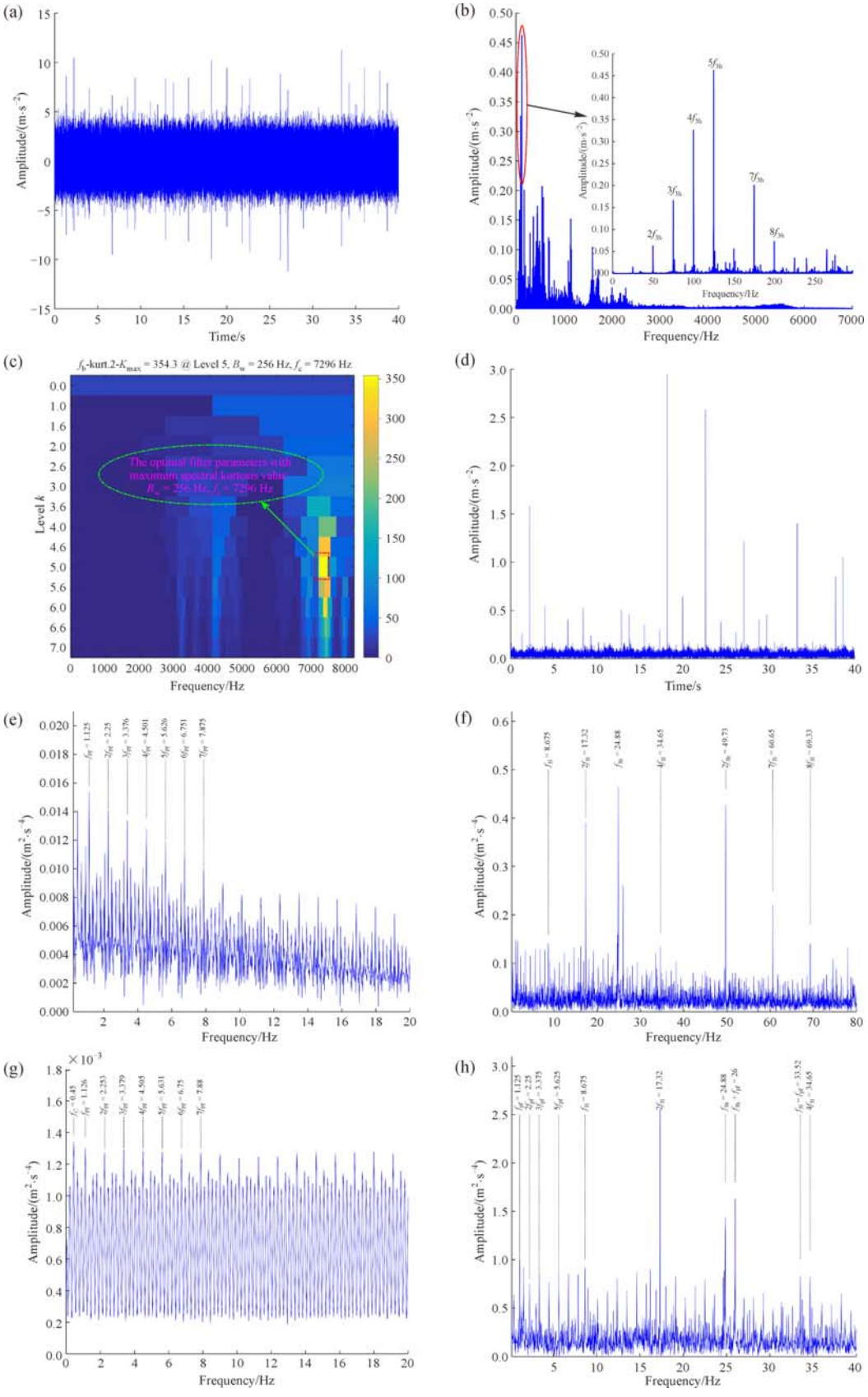

Fig. A1 Results of measurement #2: (a) Raw vibration signal; (b) its spectrum; (c) Kurtogram; (d) envelope of filtered signal based on kurtogram; (e) time wavelet energy spectrum of filtered signal; (f) the squared envelope spectrum of raw vibration signals; (g) the squared envelope spectrum of the filtered signal based on kurtogram; (h) the time wavelet energy spectrum of raw signal without any preprocessing approach

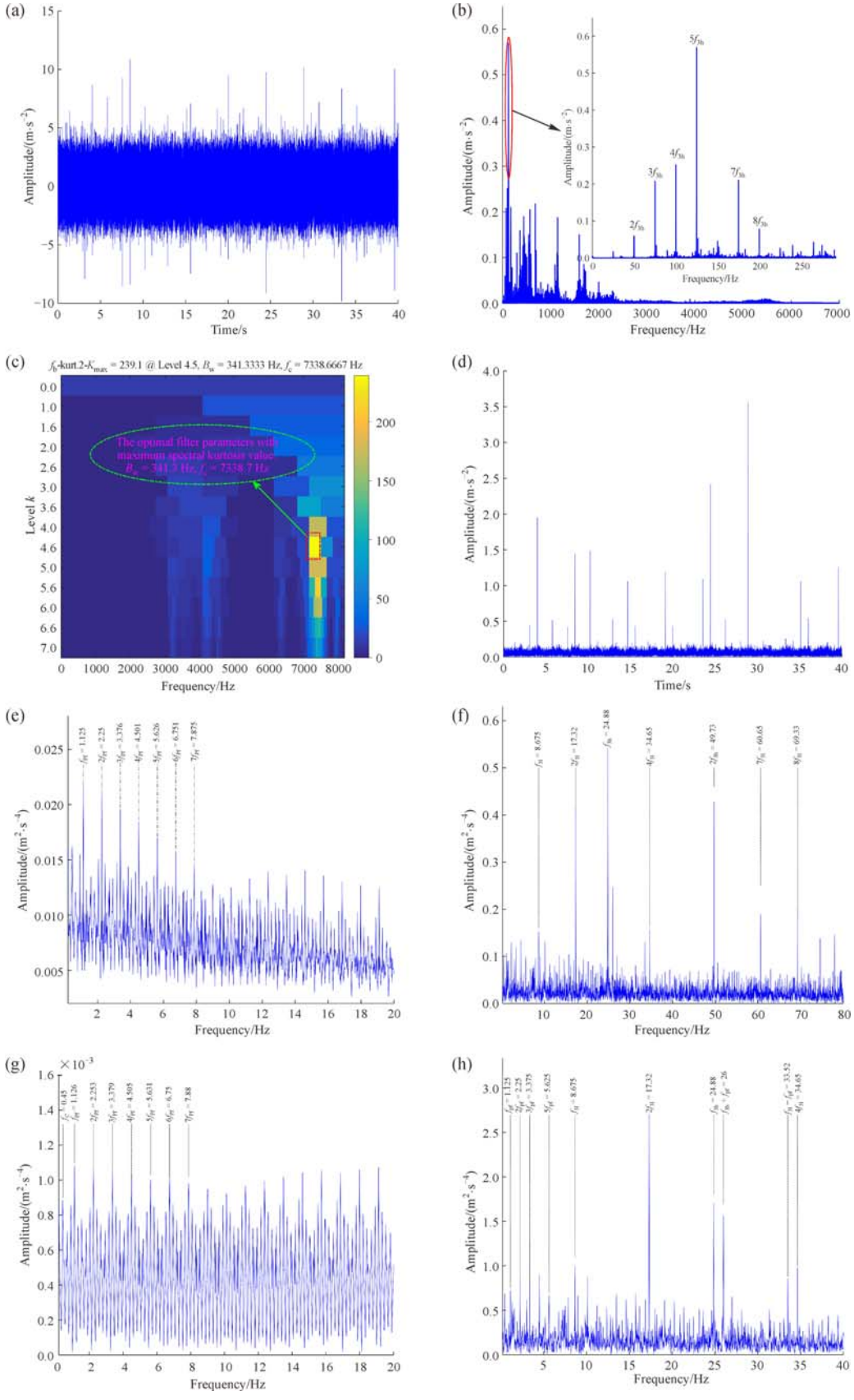

Fig. A2 Results of measurement #3: (a) Raw vibration signal; (b) its spectrum; (c) Kurtogram; (d) envelope of filtered signal based on kurtogram; (e) time wavelet energy spectrum of filtered signal; (f) the squared envelope spectrum of raw vibration signals; (g) the squared envelope spectrum of the filtered signal based on kurtogram; (h) the time wavelet energy spectrum of raw signal without any preprocessing approach

References

1. Amirat Y, Benbouzid M E H, Al-Ahmar E, et al. A brief status on condition monitoring and fault diagnosis in wind energy conversion systems. Renewable & Sustainable Energy Reviews, 2009, 13(9): 2629–2636
2. Hameed Z, Hong Y S, Cho Y M, et al. Condition monitoring and fault detection of wind turbines and related algorithms: A review. Renewable & Sustainable Energy Reviews, 2009, 13(1): 1–39
3. Feng Z, Liang M, Zhang Y, et al. Fault diagnosis for wind turbine planetary gearboxes via demodulation analysis based on ensemble empirical mode decomposition and energy separation. Renewable Energy, 2012, 47: 112–126
4. Younus A M D, Yang B S. Intelligent fault diagnosis of rotating machinery using infrared thermal image. Expert Systems with Applications, 2012, 39(2): 2082–2091
5. Toutountzakis T, Tan C K, Mba D. Application of acoustic emission to seeded gear fault detection. NDT & E International, 2005, 38(1): 27–36
6. Ottewill J R, Orkisz M. Condition monitoring of gearboxes using synchronously averaged electric motor signals. Mechanical Systems and Signal Processing, 2013, 38(2): 482–498
7. Li C, Liang M. Extraction of oil debris signature using integral enhanced empirical mode decomposition and correlated reconstruction. Measurement Science & Technology, 2011, 22(8): 085701
8. Samuel P D, Pines D J. A review of vibration-based techniques for helicopter transmission diagnostics. Journal of Sound and Vibration, 2005, 282(1–2): 475–508
9. Lei Y, Lin J, Zuo M J, et al. Condition monitoring and fault diagnosis of planetary gearboxes: A review. Measurement, 2014, 48: 292–305
10. Li C, Sanchez V, Zurita G, et al. Rolling element bearing defect detection using the generalized synchrosqueezing transform guided by time-frequency ridge enhancement. ISA Transactions, 2016, 60: 274–284
11. Cong F, Zhong W, Tong S, et al. Research of singular value decomposition based on slip matrix for rolling bearing fault diagnosis. Journal of Sound and Vibration, 2015, 344: 447–463
12. Ho D, Randall R B. Optimisation of bearing diagnostic techniques using simulated and actual bearing fault signals. Mechanical Systems and Signal Processing, 2000, 14(5): 763–788
13. Antoni J. The spectral kurtosis: A useful tool for characterizing non-stationary signals. Mechanical Systems and Signal Processing, 2006, 20(2): 282–307
14. Antoni J. Fast computation of the kurtogram for the detection of transient faults. Mechanical Systems and Signal Processing, 2007, 21(1): 108–124
15. Antoni J, Randall R B. The spectral kurtosis: Application to the vibratory surveillance and diagnostics of rotating machines. Mechanical Systems and Signal Processing, 2006, 20(2): 308–331
16. Wang Y, Liang M. An adaptive SK technique and its application for fault detection of rolling element bearings. Mechanical Systems and Signal Processing, 2011, 25(5): 1750–1764
17. Barszcz T, Randall R B. Application of spectral kurtosis for detection of a tooth crack in the planetary gear of a wind turbine. Mechanical Systems and Signal Processing, 2009, 23(4): 1352–1365
18. Lei Y, Lin J, He Z, et al. Application of an improved kurtogram method for fault diagnosis of rolling element bearings. Mechanical Systems and Signal Processing, 2011, 25(5): 1738–1749
19. Yan R, Gao R, Chen X. Wavelets for fault diagnosis of rotary machines: A review with applications. Signal Processing, 2014, 96: 1–15
20. Chen J, Li Z, Pan J, et al. Wavelet transform based on inner product in fault diagnosis of rotating machinery: A review. Mechanical Systems and Signal Processing, 2016, 70–71: 1–35
21. Lin J, Qu L. Feature extraction based Morlet wavelet and its application for mechanical fault diagnosis. Journal of Sound and Vibration, 2000, 234(1): 135–148
22. Jiang Y, Tang B, Liu W. Feature extraction method of wind turbine based on adaptive Morlet wavelet and SVD. Renewable Energy, 2011, 36(8): 2146–2153
23. Dwyer R F. Detection of non-Gaussian signal by frequency domain kurtosis estimation. In: Proceedings of the International Conference on Acoustic, Speech, and Signal Processing. Boston, 1983, 607–610
24. Wang Y, Xiang J, Markert R, et al. Spectral kurtosis for fault detection, diagnosis and prognostics of rotating machines: A review with applications. Mechanical Systems and Signal Processing, 2016, 66–67: 679–698
25. Program for the fast kurtogram provided by J. Antoni. Retrieved from https://cn.mathworks.com/matlabcentral/fileexchange/48912-fast-kurtogram
26. Chu F, Peng Z, Feng Z, et al. Modern Signal Processing Methods in Machinery Fault Diagnosis. Beijing: Science Press, 2009, 34–37 (in Chinese)